Reduced Path Successive Cancellation List Decoding for Polar Codes

Walled Khalid Abdulwahab[*], Abdulkareem Abdulrahman Kadhim

College of Information Engineering, Al-Nahrain University, Baghdad, Iraq

Abstract

Polar codes have already been adopted in 5G systems to improve error performance. Successive cancellation list (SCL) decoding is usually used at the decoder and involves lengthy processing. Therefore, different methods have been developed to reduce an SCL decoder's complexity. In this paper, a reduced path successive cancellation list (RP-SCL) decoder is presented to reduce this complexity, where some decoding paths are pruned. The pruning is achieved by using three different thresholds: two for the path metric and one for the pruning depth in the decoding tree. An optimization procedure is considered to determine the optimum settings for these thresholds. The simulation tests are carried out over models of an additive white Gaussian noise channel and a fading channel by using 5G environments. The results reveal that the proposed RP-SCL decoder provides the complexity reduction in terms of the average number of processed paths at high SNR. Additionally, the computational complexity and the memory requirements decrease.

Keywords: polar codes, SCL, tree pruning, 5G, mmWave

1. Introduction

Polar codes, introduced by Erdal Arikan in 2009, are linear block codes that utilize channel polarization to achieve the channel capacity of symmetric binary–input discrete memoryless channels (B-DMC) [1]. Polar codes with successive cancellation (SC) decoders have achieved the attractive performance for long coded block length (N) with a complexity of $O(N.\log_2 N)$ [2].

SC utilizes a binary tree for representing polar codes in the decoding process. It navigates the tree by picking the left edges until the leaf nodes are reached. If the node is a frozen one, then it is set to zero. In the case of information nodes, threshold detection is used to estimate the bit value, and SC backtracks to the right edge [3]. When a node gets the estimation values from both of its children, it combines the estimated values and pushes its own estimation to its parent node. Thus, SC navigates the whole decoding tree until all of the leaf nodes are decoded.

Unfortunately, the performance of an SC decoder is not as good as that of maximum likelihood (ML) decoding with short and moderate coding lengths, which is very important for 5G applications [4-5]. To overcome this weakness, successive cancellation list (SCL) decoding was proposed to improve the performance of polar codes for low and moderate N [6].

In the SCL approach, a set of SC decoders works together and maintains different candidate paths. At the leaf nodes and in the case of information nodes, both bit values 0 and 1 are considered, and the number of decoding paths are duplicated. This process continues, and the number of decoding paths is doubled at each information node [6]. A pruning process is used to limit the number of paths to L paths, where L is the decoding list size.

---
[*] Corresponding author. E-mail address: walled.khalid@coie-nahrain.edu.iq

Tel.: +964-770-1323837

Polar codes with an SCL decoder compete in performance with other modern channel coding schemes [7-8]. The improvement in performance achieved by SCL is at the cost of increasing the decoding complexity from $O(N.\log_2 N)$ to $O(L.N.\log_2 N)$. This represents a critical issue for most modern communication systems. Many studies have focused on reducing the SCL decoder complexity, which is substantial for 5G devices [4-5]. These works used different approaches to achieve complexity reduction.

The decoding tree path pruning approach was proposed in [9-10] to reduce the number of active decoding paths. At each decoding level, a threshold condition is determined, and any path with a metric which does not satisfy the threshold will be removed. The threshold is specified on the basis of the path metric values and a certain parameter. This parameter is determined at each decoding level depending on a list including pruned paths, which have a significant impact on the performance of the decoder. The list must be updated at each level. This list and its updating mechanism can add overhead to the decoding process.

Decoding tree partitioning represents another approach for reducing SCL decoder complexity. In [11-13], a partitioning algorithm to break down the decoding tree for SCL was proposed and developed to reduce the required memory space. In [14-16], the approaches for reducing the SCL computational complexity and latency were presented by removing the redundant and unnecessary calculations or by using the specific sub-codes and nodes in the polar code.

Most of the above-mentioned works are either concerned with reducing the memory requirement for the decoder at the cost of increasing the decoding latency, as in [11-13], or interested in reducing the computational complexity of the decoder, as in [14-16]. The decoding tree pruning approach proposed in [9-10] reduced the total number of processed paths, which in turn reduced the computational complexity, required memory, and the decoding latency. The limitation of the later works was the added overhead to the decoding process by the updating mechanism for the pruning threshold value; in addition, the proposed system was evaluated over an additive white Gaussian noise (AWGN) channel only. In this work, the idea of reducing the complexity of an SCL decoder by tree pruning was utilized. The purpose is to reduce the average number of processed paths and in turn reduces the SCL decoder complexity with the minimum added overhead. Three thresholds were considered to control the pruning of the decoding paths. These thresholds were determined on the basis of three different parameters.

The values of these parameters were optimized on the basis of a fixed value of the signal-to-noise ratio (design SNR) in order to achieve the maximum possible reduction in the decoding complexity accompanied by the minimum degradation in the BER performance. This optimization process was carried out before the actual data transmission; thus, no added overhead was required as in the previous works. The proposed decoder, which is called reduced path SCL or RP-SCL, was evaluated over an AWGN channel and a fading channel with a 5G environment. RP-SCL succeeds in achieving considerable reduction in the decoding complexity as compared to that of the standard SCL decoder.

The rest of this paper is organized as follows: In Section 2, the proposed RP-SCL decoder is described along with its complexity reduction. The considered 5G environment and channel model are presented in Section 3. The results of the proposed RP-SCL decoder over the considered channel models are presented and discussed in Section 4. Finally, the conclusions of the work are given in Section 5.

2. Proposed Reduced Path SCL Decoder

The SC and SCL decoding processes are identical in their initial steps but differ in the mechanisms of decoding the data bits. Instead of having the final decoding decision for the current data bit based on the thresholding decision used in SC, two paths are created with the two possible values for the decoded bit ('0' and '1') in the SCL decoder. Clearly, the number of paths is duplicated at each decoding step.

Consider a decoding tree for an SCL decoder with N levels and a maximum of L paths at a time. A pruning process removing the worst paths is used to limit the number of decoding paths to just L paths on the basis of the path metric (PM) defined in [17], which can be obtained by:

$$C_l^{(i)} \triangleq \sum_{j=0}^{i} \ln(1 + e^{-(1-2\hat{u}_j[l]).L_n^{(j)}[l]})$$

(1)

where $C_l^{(i)}$ is the PM of the lth path at the ith level, $\hat{u}_j[l]$ is the decoded data bit at the jth level ($0 \leq j \leq i$) and l^{th} path, n is the power of the Kronecker matrix used to generate the codeword, and $L_n^{(i)}[l]$ is the log likelihood ratio (LLR) for bit u_i defined by the following equation [17]:

$$L_l^{(i)} = \ln\left(\frac{w_n^{(i)}(y, \hat{u}^{i-1}[l] \mid 0)}{w_n^{(i)}(y, \hat{u}^{i-1}[l] \mid 1)}\right)$$

(2)

where $\hat{u}^{i-1}$ is the past route of the path and $w_n^{(i)}$, with $i \in N$ and $N = 2^n$, is a binary discreet memoryless channel with u and y as its input and output, respectively. Investigating the SCL decoding process, one may conclude that most of the correct paths are those with the least PM lying at the beginning of the list.

Table 1 illustrates the distribution of the correct paths over the SCL decoding list index for 782 transmitted codewords by using a polar code with a coded block length (N) of 256 bits and a data block length (K) of 128 bits (i.e. PC(256,128)) and with a list size of 8 for two different SNR values of 1 and 3 dB over an AWGN channel. This table clarifies that a majority of the correct paths are those associated with the low indices. The case of 3-dB SNR shows that almost all the correct paths have an index of 1.

Table 1 Number of correct paths at each list index for $L = 8$ over AWGN channel

Index	1	2	3	4	5	6	7	8
SNR = 1 dB	669	59	23	14	7	5	3	2
SNR = 3 dB	774	8	0	0	0	0	0	0

According to Table 1, the possibility of having redundant paths is high. It allows for the further pruning or discarding of a number of paths usually with a high PM without, however, affecting the performance as shown later. Thus, a reduced path SCL (RP-SCL) decoder that utilizes three thresholds is proposed in this work. These thresholds are derived on the basis of three different parameters. The optimum parameter settings are considered after a thorough investigation. The path pruning in RP-SCL is established after the SCL conventional pruning is performed. In the remaining parts of this section, the threshold values are clarified along with their parameter settings.

2.1. Reduction of terminated branches using maximum metric

In conventional SCL, the L paths are arranged according to their path metrics with the maximum path metric (C_{max}) corresponding to the worst path. Let $\{C_l\}$ be the set of path metrics of all the L paths at the given decoding level. The proposed RP-SCL decoding algorithm reduces the number of processing paths by using three different thresholds. The first threshold (T_α) is determined according to C_{max} which can be obtained by:

$$T_\alpha = C_{max} - \alpha.C_{max}, \quad 0 < \alpha < 1$$

(3)

In the RP-SCL decoding algorithm, any path with C_l which is greater than T_α is discarded. Thus, the number of discarded paths at each level is not fixed and usually depends on the value of T_α and the path metrics. Clearly, when the average number of processed paths (L_{av}) by RP-SCL is less than L, RP-SCL has an advantage over the conventional SCL decoder.

To find the optimum value of the threshold level T_α for the given code, α is varied from 0 to 1, and the corresponding L_{av} is determined. The optimal value of α (α_{opt}) corresponds to the least L_{av}. As α increases, L_{av} decreases until a turning point is reached at α_{opt}. After this point, L_{av} then starts to increase as α approaches its maximum value of unity.

The decrease in T_α is due to the high value of α results in small L_{av}. A problem may occur when all the metrics are greater than T_α so that all the paths must be pruned, which leads to a failure of the decoding process. In such a case, all the L paths are considered in the decoding process. To overcome this limitation, a new path reduction mechanism is considered, as described later (Subsection 2.3).

2.2. Reduction of decoding depth

A reduction in L_{av} usually leads to a performance degradation of the RP-SCL decoding. To reduce this degradation, the depth of the decoding tree, at which the pruning is started, is controlled by D_β where:

$$D_\beta = \lceil \beta.K \rceil, \quad 0 < \beta < 1 \tag{4}$$

where K is the length of the data block at the input of the polar encoder, and $\lceil \beta.K \rceil$ is the ceiling of $\beta.K$.

When the decoding depth reaches D_β in terms of the number of data bits, the RP-SCL pruning is executed. When the value of β is close to 0, the pruning process starts at the top of the decoding tree. Thus, a further reduction in complexity is achieved. As the value of β increases, the pruning starts at the relatively low levels of the decoding tree. When the β value is close to unity, L_{av} is increased, and the decoder performance is improved. A compromise between L_{av} and the decoding performance can be achieved to determine β_{opt}.

2.3. Reduction of terminated branches using metrics' mean

To overcome the problem mentioned in the subsection 2.1 regarding the pruning of all the paths by a small value of T_α, a third threshold level test based on the mean value of the path metrics $\bar{C}_l$ is used to reduce the decoding complexity while maintaining the acceptable performance. The new threshold, which is called T_γ, is used only for the case when the T_α threshold tests the pruning of all the paths at a given level. The threshold test of T_γ is similar to that of T_α, where any path with C_l is greater than T_γ, is pruned. The threshold level T_γ is defined as:

$$T_\gamma = \gamma.\bar{C}_l, \quad \gamma \geq 1 \tag{5}$$

Furthermore, the mean value of the metric $\bar{C}_l$ is calculated as:

$$\bar{C}_l = \frac{\sum_{j=1}^{L} C_j^{(i)}}{L} \tag{6}$$

where i is the decoding level. The effect of T_γ on the RP-SCL pruning process is controlled by the parameter γ. As γ increases, L_{av} increases, and the decoder performance improves. In contrast, when γ decreases, L_{av} decreases at the cost of performance degradation. Because α_{opt} usually achieves a good reduction in L_{av} at the cost of noticeable performance degradation, the range of γ is considered to be ≥ 1 in order to mitigate the effect of α_{opt} on the decoder performance. The optimum setting of γ depends on both the complexity (L_{av}) and the bit error rate (BER) performance of the decoder.

2.4. Full operation of the proposed RP-SCL decoder

The operation of the RP-SCL decoder relies on determining the optimum values for the three parameters (α, β, and γ) at the assumed SNR (called design SNR) prior to any transmission, as shown in algorithm 1. When the actual transmission

begins, RP-SCL uses the optimum parameters to determine the threshold tests in order to use them in the decoding process, as described previously.

The optimum values of α, β, and γ are determined by varying their values according to the given ranges and then selecting the value that produces the least L_{av} as follows: First, α_{opt} is determined, while β and γ are set to 0 and 1, respectively. Then, α_{opt} along with $\gamma = 1$ is used to determine β_{opt}. Finally, the value of γ_{opt} is determined, while α and β are set to their optimum values α_{opt} and β_{opt}, respectively. A simplified block diagram of the data transmission system with the related components of the polar coding and decoding is shown in Fig. 1.
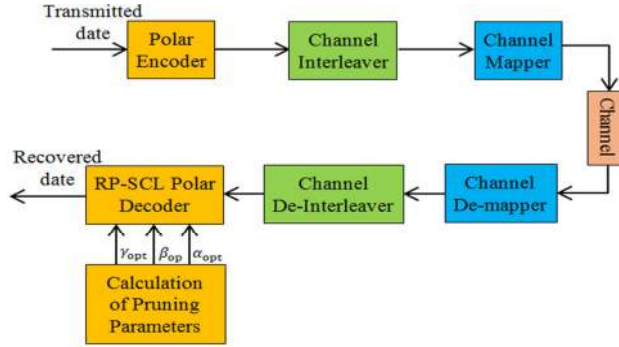

Fig. 1. The simplified block diagram of the data transmission system

Algorithm 1 The determination of the optimum pruning parameters and the operation of RP-SCL

// Parameter setting phase, determining the optimum values for the pruning parameters on the basis of specific design SNR
// Steps for determining α_{opt}
1   $\beta = 0$, $\gamma = 1$, $0 < \alpha < 1$, $c_1 = 1$ // c_1: index for $L_{av\alpha}$ vector
2   for $j = 0.1:0.1:\alpha_M$ do   // α_M: maximum value for α
3       $L_{avj} \leftarrow$ Call RP-SCL (N, K, R_N, α_j, β, γ)   // R_N: Received coded vector of length N
4       $L_{av\alpha}(c_1) = L_{avj}$ // $L_{av\alpha}$: vector holds L_{av} values over the range of α
5       $c_1 = c_1 + 1$
6   End for
7   $\alpha_{opt} \leftarrow \min(L_{av\alpha})$
// Steps for determining β_{opt}
8   $\alpha = \alpha_{opt}$, $\gamma = 1$, $0 \leq \beta < 1$, $c_2 = 1$ // c_2: index for $L_{av\beta}$ and BER_{β} vector
9   for $j = 0:0.1:\beta_M$ do   // β_M: maximum value for β
10      $[d_r, L_{avj}] \leftarrow$ Call RP-SCL(N, K, R_N, α_{opt}, β_j, γ)   // d_r: received data
11      $BER_{\beta}(c_2) = compare$ (d_s, d_r)   // d_s: sent data, BER_{β}: vector holds BER values over the range of β
12      $L_{av\beta}(c_2) = L_{avj}$ // $L_{av\beta}$: vector holds L_{av} values over the range of β
13      $c_2 = c_2 + 1$
14 End for
15 $\beta_{opt} \leftarrow$ Compromise ($L_{av\beta}$, BER_{β})   // Determine β_{opt} on the basis of compromise between $L_{av\beta}$ and BER_{β}
// Steps for determining γ_{opt}
16 $\alpha = \alpha_{opt}$, $\beta = \beta_{opt}$, $\gamma \geq 1$, $c_3 = 1$ // c_3: index for $L_{av\gamma}$ and BER_{γ} vector
17 for $\gamma_j = 1:0.025:\gamma_M$ do   // γ_M: maximum value for γ
18      $[d_r, L_{avj}] \leftarrow$ Call RP-SCL(N, K, R_N, α_{opt}, β_{opt}, γ_j)
19      $BER_{\gamma}(c_3) = compare$ (d_s, d_r)   // BER_{γ}: vector holds BER values over the range of γ
20      $L_{av\gamma}(c_3) = L_{avj}$ // $L_{av\gamma}$: vector holds L_{av} values over the range of γ
21      $c_3 = c_3 + 1$
23 End for
24 $\gamma_{opt} \leftarrow$ Compromise ($L_{av\gamma}$, BER_{γ})   // Determine γ_{opt} on the basis of compromise between $L_{av\gamma}$ and BER_{γ}
// Actual transmission phase, SCL decoding process
25 $[d_r, L_{av}] \leftarrow$ RP-SCL(N, K, R_N, α_{opt}, β_{opt}, γ_{opt})   // L_{av}: average number of processed paths with RP-SCL decoding

---

Subroutine 1 RP-SCL(N, K, R_N, α_{opt}, β_{opt}, γ_{opt})

---

1   $c_4 = 1$ // c_4: vector index
2   For $i = 1, 2, …, N$, do   // N: coding length
3   If $i \in F$ then   // F: Frozen bit set

4	$\forall\,\ell\,\epsilon\,\mathcal{L}$, Update $(C_\ell^{(i)})$ and $\hat{u}_\ell^{(i)} = 0$, no path duplicate	// $\mathcal{L}$: set of active paths, ℓ: path $\epsilon\,\mathcal{L}$
		// $C_\ell^{(i)}$: path metric value according to (1), $\hat{u}$: decoded bits
5	Else	// Information bits
6	$\forall\,\ell\,\epsilon\,\mathcal{L}$, Duplicate Path (ℓ)	
7	If $|\,\mathcal{L}\,| > L$ then	
8	$l=$ length($\mathcal{L}$)	// Start conventional SCL path pruning process
9	for $j = 1, 2, \dots, l$	// l: number of current paths
10	Find $(C_j^{(i)})$	// $C_j^{(i)}$: path metric value for path j at level i determined according to (1)
11	End for	
12	$\forall\,\ell\,\epsilon\,\mathcal{L}$, sort ℓ in ascending order according to C	
13	$\mathcal{L} = $ (start: end $-$ L)	// Keep the L most likely paths, End of conventional SCL path pruning process
14	$D_\beta = \lceil \beta_{opt} . K \rceil$	// K: data block size, Start RP-SCL pruning process
15	if $\alpha_{opt} \neq 0$ and $i \geq D_\beta$	
16	$T_\alpha = \text{Max}\,(\{C^i\}) - \alpha_{opt} * \text{Max}(\{C^i\})$	
17	for $j = 1, 2, \dots, L$ do	// L: SCL list size
18	if $C_j^{(i)} \leq T_\alpha$ then	
19	$\mathcal{L}_t \leftarrow \ell_j$	// $\mathcal{L}_t$: temporary vector hold survivor paths
20	End if	
21	End for	// End pruning process on the basis of T_α thresholding
22	if $\mathcal{L}_t \neq \emptyset$ then	
23	$\mathcal{L} = \mathcal{L}_t$	
24	$\mathcal{L}_c\,(c_4) = \text{paths\_no}(\mathcal{L}_t)$	// count the number of active paths, $\mathcal{L}_c$: hold the number of active //paths at each decoding level
25	$c_4 = c_4 + 1;$	
26	Else	
27	$T_\gamma = \gamma_{opt} . \text{mean}\,(\{C^i\})$	
28	for $j = 1, 2, \dots, L$ do	// Start RP-SCL pruning on the basis of T_γ thresholding
29	if $C_j^{(i)} \leq T_\gamma$ then	
30	$\mathcal{L}_t \leftarrow \ell_j$	
31	End if	
32	End for	// End pruning process on the basis of T_γ thresholding
33	$\mathcal{L} = \mathcal{L}_t$	
34	$\mathcal{L}_c\,(c_4) = \text{paths\_no}(\mathcal{L}_t)$	
35	$c_4 = c_4 + 1;$	
36	End if	
37	End if	
38	End if	
39	End if	
40	End for	
41	$d_r = \text{CRC}\,(\mathcal{L})$	// use CRC to select the correct path among L likely paths
42	$L_{av} = \text{mean}\,(\mathcal{L}_c)$	

3. 5G Environments and Channel Model

5G system environments and channel models were used in the work to evaluate the BER performance of the proposed RP-SCL decoder. The main features of the 5G transmission system were the use of the following: millimetre wave (mmWave) frequency band, orthogonal frequency division multiplexing (OFDM), multilevel phase shift keying (MPSK) or multilevel quadrature amplitude modulation (MQAM), and multi-input multi-output (MIMO) technology [18-22].

The related parameters for the mentioned techniques actually used in the simulation are presented in Table 2. The related components of these techniques are presented within the signal mapping and de-mapping blocks of Fig. 1. The justification for the used parameter values and details of their settings could be found elsewhere [20, 23].

The channel model considered here was approved by 3GPP and defined over the frequency range of 0.5 GHz to 100 GHz for the maximum bandwidth of 2 GHz [24]. Model D (indoor office with a short delay profile) was considered using the tapped delay line channel model. The simulation parameters of the fading channel model are given in Table 3.

Table 2 The simulation parameters of 5G transmission system

Parameter	Value or Type
Carrier Frequency	28 GHz
Bandwidth	50 MHz
Modulation	QPSK
No. of Subcarriers in OFDM	512
Length of Cyclic Prefix	36
Sub-Carrier Spacing	120 kHz
OFDM Frame Duration	8.33 μs
MIMO Type	4×4 (STBC)

Table 3 The simulation parameters of fading channel model

Parameter	Value
No. of Multipaths	3
Path Gains	[−0.2 −18.8 −21] dB
Normalized Path Delay	[0 0.035 0.612]
Delay Spread	16 ns
K-Factor	13.3 dB
Velocity	3 km/h
Max. Doppler Shift	77.784 Hz

4. Performance Evaluation of RP-SCL Decoder

The proposed RP-SCL decoder was used for polar code PC(256, 128) with two list sizes of 8 and 32. The selected block length for the polar code was among the interesting lengths in two 5G use cases: the massive machine type communication (mMTC) and the ultra-reliable low latency (URLL) [25]. RP-SCL with the considered polar code was simulated by using QPSK and OFDM modulation with the related transmission parameters, as shown in Table 2.

Two channel models are used: the additive white Gaussian noise (AWGN) channel and a fading channel model in the mmWave frequency band-related specifications, as shown in Table 3. The proposed RP-SCL decoder together with the conventional SCL decoder is simulated by using Matlab R2019a version 9.6. The results of the simulation are presented in this section followed by the discussions related to the computational complexity and the memory requirements of RP-SCL.

4.1. Simulation tests and results

The extensive simulation tests are conducted in this work which covers the estimation of the optimum pruning parameters for each channel and the performance evaluation of the proposed RP-SCL decoder together with that of the standard SCL decoder for the sake of comparison. For the AWGN channel, an SNR of 3.1 dB is considered the design SNR to determine the optimum pruning parameters, where the SCL decoder for the adopted polar code achieves a BER of 10^{-4}. This BER value is considered to be acceptable here. The corresponding SNR for the fading channel is approximately 24.25 dB.

The estimation of the optimum pruning parameters started by finding α_{opt} first as mentioned before. This is followed by determining β_{opt} and finally γ_{opt} over each channel. Fig. 2 illustrates the variation of L_{av} against α with $L = 8$. The value of α that yields the minimum L_{av} (α_{opt}) is approximately 0.6 with an average number of processed paths of 4.2.
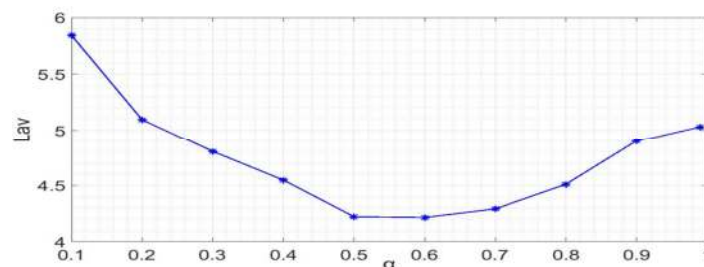

Fig. 2 L_{av} *vs.* α with $L = 8$ over AWGN

Fig. 3 demonstrates the variation of BER and L_{av} against β for the list size of 8, with α set to its optimum value (α_{opt}). The value of L_{av} for the proposed RP-SCL decoder is close to L at β values above 0.7. Therefore, the considered range of β is limited to 0.7 for all the tests. When β is increased, the BER decays smoothly, while L_{av} increases. As a compromise between the complexity (L_{av}) and the BER performance, the value of β at the intersection point of the two curves in Fig. 3 is considered the optimum value.

Thus, β_{opt} is taken to be 0.36 for $L = 8$. Both α_{opt} and β_{opt} are considered for determining γ_{opt}. Fig. 4 shows the decoder behavior in terms of BER and L_{av} with different values of γ over the range of 1 to its maximum value of 1.2 (if above this value, L_{av} is close to $L = 8$). As for the selection of β_{opt}, γ_{opt} is the value of γ at the intersection point of the two curves, which is 1.14 in this case.
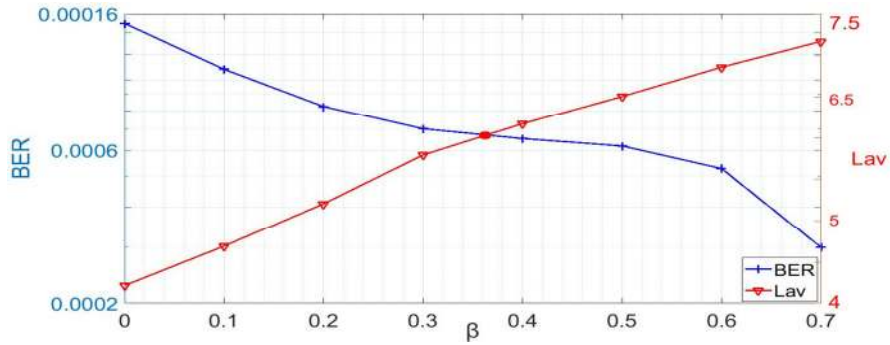

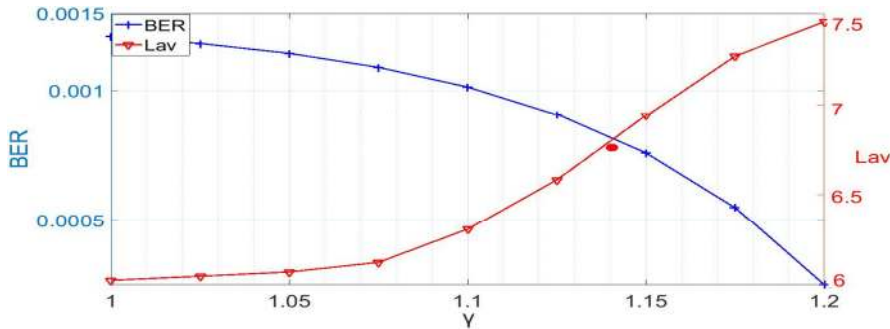Fig. 3 BER and L_{av} vs. β with $L = 8$ over AWGN

Fig. 4 BER and L_{av} vs. γ with $L = 8$ over AWGN

The same tests as those used to determine α_{opt}, β_{opt}, and γ_{opt} values for AWGN using $L = 8$ are performed to determine the corresponding values for the AWGN channel with $L = 32$ and for the fading channel with both $L = 8$ and 32. The obtained optimum parameters are shown in Table 4.

Table 4 The RP-SCL optimum parameters for AWGN and fading channels.

Parameter	AWGN Channel		Fading Channel	
	$L = 8$	$L = 32$	$L = 8$	$L = 32$
α_{opt}	0.6	0.6	0.5	0.6
β_{opt}	0.36	0.25	0.379	0.345
γ_{opt}	1.14	1.1025	1.117	1.0825

After the determination of the optimum value of each pruning parameter, the full operation of the proposed RP-SCL decoder proceeds as described in Section 2. The role of the RP-SCL decoder in reducing the complexity is depicted in Figs. 5-6 for the AWGN channel and the fading channel, respectively.

Each of these figures illustrates the complexity of the RP-SCL decoder in terms of the average processed paths (L_{av}) in the decoding against the SNR given by E_b/N_o in decibels. Fig. 5 depicts that L_{av} is reduced by 2 and 12.5 for $L = 8$ and 32 over the AWGN channel, respectively, at a high SNR. The corresponding values for the fading channel, shown in Fig. 6, are 1.8 and 10 for $L = 8$ and 32, respectively.
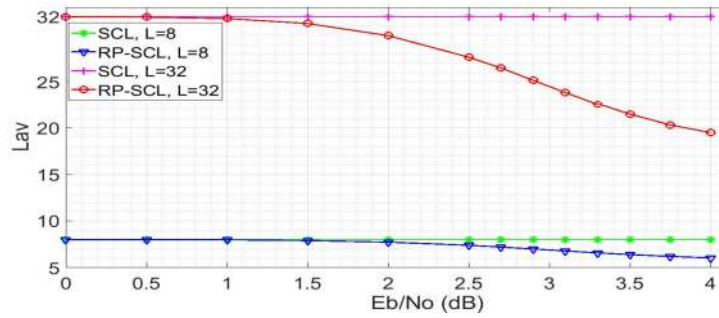
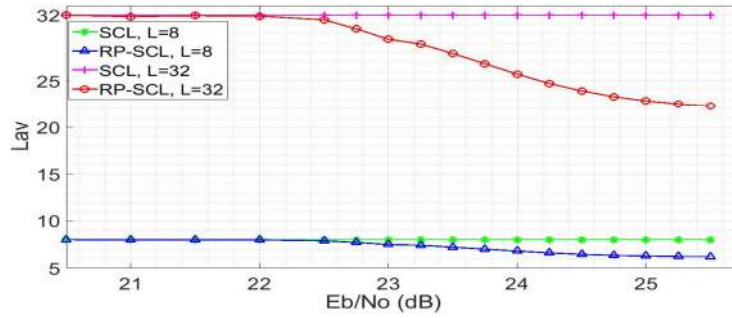Fig. 5 The variation of L_{av} with E_b/N_0 over AWGN channel

Fig. 6 The variation of L_{av} with E_b/N_0 over fading channel

The results, which are presented in Table 4, demonstrates that α_{opt} is less sensitive to the changed list size and channel than the other two pruning parameters (β_{opt} and γ_{opt}). In addition, the results reveal that α_{opt} is the most important parameter for achieving the decoder complexity reduction, as shown in Fig. 2, where for $L = 8$ over the AWGN channel, L_{av} is reduced to 4.2 paths at the cost of increasing the BER to 10^{-3}. In contrast, the main role of the other pruning parameters β_{opt} and γ_{opt} is to mitigate the effect of α_{opt} on the performance, where the BER is reduced to the 10^{-4} range, as demonstrated in Fig. 7 with the increase of L_{av}, 6, for $L = 8$ over the AWGN channel.
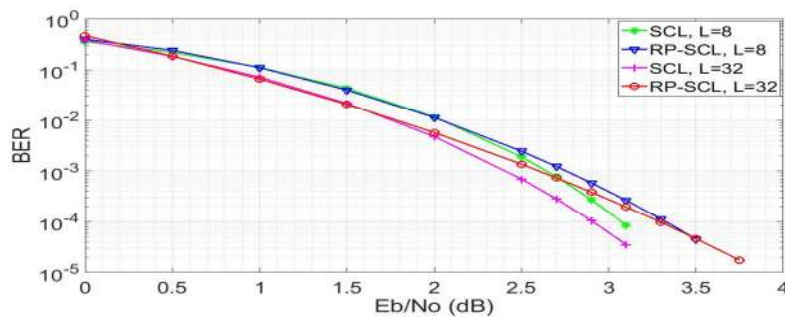

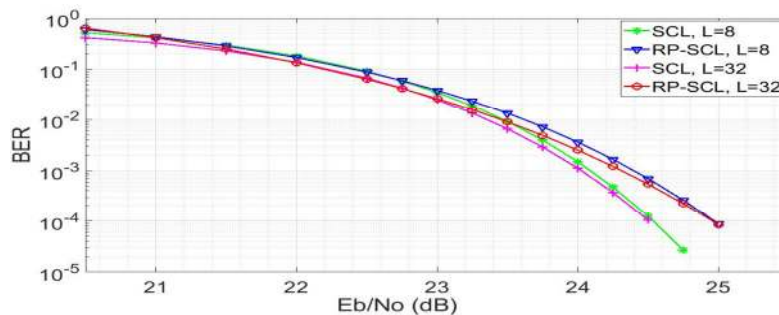Fig. 7 The BER performance of different decoders over AWGN channel

Fig. 8 The BER performance of different decoders over fading channel

Figs. 7 and 8 show the BER performance of the SCL and the RP-SCL decoders over the AWGN channel and the fading channel, respectively. The BER performance of RP-SCL is close to that of SCL at a low SNR, while relatively small degradations occurrs at a high SNR for the two channels and list sizes used. This degradation for the AWGN channel corresponds to 0.3 and 0.4 dB for the list sizes of 8 and 32, respectively, at the BER of 10^{-4}, as depicted in Fig. 7.

The corresponding degradation for the fading channel is approximately 0.35 and 0.4 dB for the list sizes of 8 and 32, respectively, as shown in Fig. 8. Such degradation can be considered to be the cost paid for the complexity reduction of RP-SCL as compared to SCL.

4.2. Complexity of the proposed RP-SCL decoder

The performance evaluation of the proposed RP-SCL decoder together with its complexity is summarized in Table 5 for all the considered channels and list sizes. As the complexity of the SCL and RP-SCL is mainly determined by the number of processed paths, the overall reduction in L_{av} for the RP-SCL decoder as compared to that in L for the SCL decoder determines the percentage of computational complexity reduction ($CCR\%$) of the RP-SCL decoder. The value of $CCR\%$ can be calculated as:

$$CCR\% = \frac{L - L_{av}}{L} * 100\% \tag{7}$$

where L is the list size of the SCL decoder, and L_{av} is the average number of paths processed by the RP-SCL decoder.

Table 5 The summary of the performance comparison of RP-SCL and SCL decoders

	Compared term relative to that of standard SCL decoder	$L = 8$	$L = 32$
AWGN Channel	Percentage reduction in L_{av} (RCC%)	25%	40%
	SNR degradation in dB at BER = 10^{-4}	0.3	0.4
Fading Channel	Percentage reduction in L_{av} (RCC%)	22.5%	30.5%
	SNR degradation in dB at BER = 10^{-4}	0.35	0.4

Clearly, Table 5 depicts the considerable complexity reduction of the proposed RP-SCL over SCL for both the channels and the list sizes. This reduction for the list size of 8 ranges from 22.5% for the fading channel to 25% for the AWGN channel. The corresponding reduction for the list size of 32 is considerably larger. The corresponding degradation in the SNR requires to achieve a BER of 10^{-4} ranged from 0.3 to 0.4 dB over all the considered channels and list sizes.

The computational complexity for a general polar code PC(N, K) with an SCL decoder having a list size of L is O($L.N.\log_2 N$) [2]. As the proposed decoder reduces the required L to L_{av} on average, one might conclude that the computational complexity of the proposed RP-SCL decoder is roughly O($L_{av}.N.\log_2 N$).

Algorithm 1 shows that the additional mathematical operations required by the RP-SCL decoder are as follows: four multiplications, L additions, and ($2L + 3$) comparisons in the worst case for each decoding level. The required operations to determine the optimum parameters (α_{opt}, β_{opt}, and γ_{opt}) of the proposed RP-SCL decoder can be carried out prior to the actual transmission and do not affect the decoding operations.

It has been shown that the expression used to estimate the total memory required for SCL decoder is as follows [12]:

$$M_{SCL} = \left[N + L(N - 1) \right] Q_{LLR} + L Q_{PM} + L(2N - 1) \tag{8}$$

where M_{SCL} is the total memory size (in bits) for the SCL decoder, Q_{LLR} is the number of bits used to quantize LLR, and Q_{PM} is the number of bits required to quantize the path metrics PM. For the proposed RP-SCL decoder, one may use the same expression with L replaced by L_{av} to calculate the required memory of the RP-SCL decoder as follows:

$$M_{RP-SCL} = \left[N + L_{av}(N - 1) \right] Q_{LLR} + L_{av} Q_{PM} + L_{av}(2N - 1) \tag{9}$$

where M_{RP-SCL} is the total required memory for the proposed RP-SCL decoder.

5. Conclusions

A low-complexity decoder for polar codes was proposed in this paper. The proposed decoding algorithm, which is called reduced path successive cancellation list (RP-SCL), relies on the pruning of the decoding paths. Three parameters were used to control the pruning thresholds, which were used to perform the path pruning resulting in a considerable reduction in the decoder complexity with a slight degradation in the BER performance. These parameters were optimized to achieve the best results in terms of the complexity reduction and the least BER performance loss. The optimization was performed over the models of AWGN and mmWave fading channels. The parameters were optimized prior to the transmission so that no extra processing was required during the actual transmission. The simulation results of RP-SCL showed that a relatively high complexity reduction was achieved at a high SNR. A reduction in the complexity of up to 40% in comparison with that of the conventional SCL decoder was obtained. A similar order achieved in the required memory and computational complexity of the decoder. Such advantages were achieved on the expense of less than 0.4 dB SNR penalty. The implementation of RP-SCL represents a challenge to assess its suitability in practice.

Conflicts of Interest

The authors declare no conflict of interest.

References

[1] E. Arikan, "Channel Polarization: A Method for Constructing Capacity-Achieving Codes for Symmetric Binary-Input Memoryless Channels," IEEE Transaction on Information Theory, vol. 55, no. 7, pp. 3051-3073, July 2009.

[2] H. Vangala, E. Viterbo, and Y. Hong, "A Comparative Study of Polar Code Constructions for the AWGN Channel," http://arxiv.org/abs/1501.02473, January 11, 2015. (under revision)

[3] P. Giard, C. Thibeault, and W. J. Gross, High-Speed Decoders for Polar Codes, Springer International Publishing, 2017.

[4] P. Marsch, Ö. Bulakç, O. Queseth, and M. Boldi, 5G System Design Architectural and Functional Considerations and Long Term Research, John Wiley & Sons Ltd, 2018.

[5] D. Chandramouli, R. Liebhar, and J. Pirskanen, 5G for the Connected World, John Wiley & Sons Ltd, 2019.

[6] I. Tal and A. Vardy, "List Decoding of Polar Codes," IEEE Transactions on Information Theory, vol. 61, no. 5, pp. 2213-2226, May 2015.

[7] W. Abdulwahab and A. Kadhim, "Comparative Study of Channel Coding Schemes for 5G," Proceedings 2018 International Conference on Advanced Science and Engineering, IEEE Press, October 2018, pp. 239-243.

[8] V. Bioglio, C. Condo, and I. Land, "Design of Polar Codes in 5G New Radio," IEEE Communications Surveys and Tutorials (Early Access), January 2020.

[9] K. Chen, K. Niu, and J. Lin, "A Reduced-Complexity Successive Cancellation List Decoding of Polar Codes," Proceedings 2013 IEEE 77th Vehicular Technology Conference (VTC Spring), IEEE Press, June 2013, pp. 1-5.

[10] K. Chen, B. Li, H. Shen, J. Jin, and D. Tse, "Reduce The Complexity of List Decoding of Polar Codes by Tree-Pruning," IEEE Communication Letter, vol. 20, no. 2, pp. 204-207, February 2016.

[11] S. Hashemi, A. Balatsoukas-Stimming, P. Giara, C. Thibeaul, and W. Gross W, "Partitioned Successive-Cancellation List Decoding of Polar Codes," Proceedings of 2016 IEEE International Conference on Acoustics, Speech and Signal Processing, IEEE Press, Shanghai, China, March 2016, pp. 957-960.

[12] S. Hashemi, M. Mondelli, S. Hassani, R. Urbanke, and W. Gross, "Partitioned List Decoding of Polar Codes: Analysis and Improvement of Finite Length Performance," Proceedings of IEEE Global Communications Conference, IEEE Press, December 2017, pp. 1-7.

[13] S. Hashemi, M. Mondelli, S. Hassani, C. Condo, R. Urbanke, and W. Gross, "Decoder Partitioning: Towards Practical List Decoding of Polar Codes," IEEE Transaction on Communication, vol. 66, no. 9, pp. 3749-3759, September 2018.

[14] S. Hashemi, C. Condo, and W. Gross, "Simplified Successive-Cancellation List Decoding of Polar Codes," Proceedings of 2016 IEEE International Symposium on Information Theory, IEEE Press, July 2016, pp. 815-819.

[15] S. Hashemi, C. Condo, and W. Gross, "Fast Simplified Successive-Cancellation List Decoding of Polar Codes," Proceedings 2017 IEEE Wireless Communications and Networking Conference Workshops, IEEE Press, March 2017, pp. 1-6.

[16] C. Condo, V. Bioglio, and I. Land, "Generalized Fast Decoding of Polar Codes," Proceedings of 2018 IEEE Global Communications Conference, IEEE Press, December 2018, pp. 1-6.

[17] A. Balatsoukas-Stimming, M. Parizi, and A. Burg, "LLR-Based Successive Cancellation List Decoding of Polar Codes," IEEE Transaction on Signal Processing, vol. 63, no. 19, pp. 5165-5179, October 2015.

[18] Z. Gao, L. Dai, D. Mi, Z. Wang, M. A. Imran, and M. Z. Shakir, "MmWave Massive MIMO Based Wireless Backhaul for 5G Ultra-Dense Network," IEEE Wireless Communication, vol. 22, no. 5, pp. 13-21, October 2015.

[19] C. Yen and C. Liu, "Hybrid OFDM/OOK Modulations in OCDMA Scheme for Free Space Optics," Proceedings of Engineering and Technology Innovation, vol. 3, pp. 01-03, August 2016.

[20] 3rd Generation Partnership Project, "5G; NR; Physical Channels and Modulation," TS 38.211 version 15.8.0 Release, July 15, 2018.

[21] A. Zaidi, R. Baldemair, V. Moles-Cases, N. He, K. Werner, and A. Cedergren, "OFDM Numerology Design for 5G New Radio to Support IoT, eMBB, and MBSFN," IEEE Communication Standard Magazine, vol. 2, no. 2, pp. 78-83, June 2018.

[22] Vishwaraj and L. Ali, "Hybrid MIMO-OFDM System for 5G Network Using VLC-A Review," Proceedings of 2019 IEEE International Conference on Electrical, Computer and Communication Technologies, February 2019, pp. 1-5.

[23] 3rd Generation Partnership Project, "5G; NR; User Equipment (UE) Radio Transmission and Reception; Part 2: Range 2 Standalone," TS 38.101-2 version 15.8.0 Release 15, January 2020.

[24] 3rd Generation Partnership Project, "5G; Study on Channel Model for Frequencies from 0.5 to 100 GHz," TR 38.901 version 14.1.1 Release, August 14, 2017.

[25] A. Sharma and M. Salim, "Polar Code: The Channel Code Contender for 5G Scenarios," Proceedings of 2017 International Conference on Computer, Communications and Electronics (Comptelix), IEEE Press, July 2017, pp. 676-682.